DOI: 10.5327/Z2317-4889201400010009

ARTICLE

Morphological and compositional variations of zircon and their metallogenetic implications: the example of the Jamon, Serra dos Carajás and Velho Guilherme suites, Amazonian Craton

Variação morfológica e composicional de zircão e suas implicações metalogenéticas: o exemplo das suítes Jamon, serra dos Carajás e Velho Guilherme, Cráton Amazônico

Claudio Nery Lamarão[1,2]*, Joseanna dos Santos Silva[2], Régis Munhoz Krás Borges[1,2], Roberto Dall'Agnol[1,2]

ABSTRACT: Zircon from granites of the Jamon suite (JS), Serra dos Carajás suite (SCS) and Velho Guilherme suite (VGS) were studied by scanning electron microscope (SEM) through backscattered electron and cathodoluminescence images and energy dispersive spectroscopy (EDS) analyses. Granites and greisens of the VGS have predominantly anhedral zircons that are altered and intensely corroded, are enriched in Hf and have the lowest Zr/Hf ratios of the studied suites. In the granites, these ratios decrease towards the more evolved varieties. Zircons of the JS are euhedral to subhedral, zoned and slightly altered; they are also comparatively depleted in Hf and display the highest Zr/Hf ratios, indicating limited potential for tin-associated mineralization. Zircons from granites of the SCS are subhedral to anhedral, altered and corroded, and show Hf contents and Zr/Hf ratios intermediate to those of the JS and VGS. The granites of the VGS with Sn-, Ta- and W-associated mineralization contain zircons with Zr/Hf ratios varying from 7 to 22. It is concluded that ratios of similar magnitude can be used as a prospecting guide for specialized granites. Zircons from the greisens associated with the Cigano granite of the SCS have average Zr/Hf ratios of approximately 23, but no cassiterite was found in these rocks, indicating that the zircons preserved their magmatic geochemical signature. This study distinguished the three granitic suites in terms of zircon composition and demonstrated the importance of their geochemical signature, especially in terms of their Zr/Hf ratio, in the identification of specialized granites. EDS-SEM analysis can thus be used in a preliminary assessment of the metallogenic potential of tin granites.

KEYWORDS: granitic suites; zircon; SEM techniques; cassiterite; Zr/Hf ratio.

RESUMO: *Zircões de granitos das Suítes Jamon (SJ), Serra dos Carajás (SSC) e Velho Guilherme (SVG) foram estudados em MEV por meio de imagens de elétrons retroespalhados e catodoluminescência e análises pontuais por EDS. Granitos e greisens da SVG apresentam zircões dominantemente anédricos, alterados e intensamente corroídos, enriquecidos em Hf e com as mais baixas razões Zr/Hf, as quais nos granitos tendem a decrescer no sentido das fácies mais evoluídas. Zircões da SJ são euédricos a subédricos, zonados e pouco alterados, comparativamente empobrecidos em Hf e com as mais elevadas razões Zr/Hf, indicando potencial reduzido para geração de mineralização estanífera. Zircões dos granitos da SSC são subédricos a anédricos, alterados e corroídos e com conteúdos de Hf e razões Zr/Hf intermediárias a dos zircões das SJ e SVG. Granitos da SVG com mineralizações de Sn, W e Ta apresentam zircões com razões Zr/Hf entre 7 e 22. Conclui-se que razões desta ordem podem ser utilizadas como guia prospectivo de granitos especializados. Por outro lado, zircões de greisens associados ao Granito Cigano da SSC apresentaram razão Zr/Hf média em torno de 23, porém nenhuma cassiterita foi encontrada nessas rochas. Isto indica que estes zircões preservaram sua assinatura magmática original. O estudo desenvolvido permitiu distinguir as três suítes graníticas em termos de composição de zircão, e mostrou a importância da assinatura geoquímica desse mineral, sobretudo da razão Zr/Hf, na identificação de granitos especializados. Análises de zircões por MEV-EDS podem, portanto, ser utilizadas na avaliação preliminar do potencial metalogenético de granitos estaníferos.*

PALAVRAS-CHAVE: *suítes graníticas; zircão; análises de MEV; cassiterita; razão Zr/Hf.*

[1]Grupo de Pesquisa Petrologia de Granitoides, Instituto de Geociências, Universidade Federal do Pará - UFPA, Belém (PA), Brazil. *E-mail: lamarao@ufpa.br; munhoz@ufpa.br; robdal@ufpa.br*

[2]Programa de Pós-Graduação em Geologia e Geoquímica, Instituto de Geociências, Universidade Federal do Pará - UFPA, Belém (PA), Brazil. *E-mail: joseanna@ufpa.br*

*Corresponding author

Manuscrito ID 30016. **Recebido em:** 24/07/2013. **Aprovado em:** 26/02/2014

INTRODUCTION

Zircon is a mineral with a high chemical resistance that is often used in dating rocks, characterizing magmatic sources, determining the degree of magmatic fractionation and studying provenance. Zircon crystals often show great morphological and textural variation, which can aid in the understanding of their geological history and, by extension, that of their host rocks. Backscattered electron (BSE) and cathodoluminescence (CL) images obtained in a scanning electron microscope (SEM) stand out among techniques used to study these variations. BSE differentiates between mineral phases due to the variation of the atomic number of the elements that constitute the mineral and the variation in density contrast. The higher the atomic number of the element present in the sample, the clearer the final image. This type of image is very useful, particularly in studying zonation in accessory minerals (Krinsley & Manley 1989; Paterson *et al.* 1989). CL is used as a petrological tool as certain minerals, including zircon, exhibit CL when bombarded with electrons. The use of these two techniques has allowed the identification of (1) distinct patterns of zoning, a feature typical of magmatic zircon and which indicate variations in the concentrations of Zr, Si, Hf, Y, P, Th, U, REE, Ca and other elements present in the crystal structure of the zircon (Hanchar & Miller 1993; Hanchar & Hudnick 1995; Fowler *et al.* 2002); (2) inherited cores in magmatic zircons, which are surrounded by overgrowths (Paterson *et al.* 1992b; Vavra *et al.* 1996); (3) modifications caused during the later and/or post-magmatic stages such as an interruption of zoning, which can cause an appearance of patches and irregular edges enriched in certain components (*e.g.*, Hf and Ca) and (4) the presence of xenocryst inclusions (*i.e.*, apatite or garnet) or mineral phases introduced after the formation of the zircon crystal (*i.e.*, thorite, xenotime, cassiterite, monazite or fluorite). Punctual chemical analyses by SEM-EDS (energy dispersive spectroscopy) or electron microprobe are essential for the identification of compositional variations in zircons. However, it has been demonstrated that zircons of specialized granites have a significant enrichment of Hf, Y, Th, U and Ca, and have low Zr/Hf ratios, indicating that the composition of zircons can be a useful guide for the preliminary assessment of the metallogenic potential of tin-mineralized granites and associated metals (Wang *et al.* 2000; Kempe *et al.* 2004; Lamarão *et al.* 2007, 2010, 2012).

Three main Paleoproterozoic A-type granite suites with ages between 1.89 and 1.86 Ga (Tab. 1), outcropping in the Carajás Province, Amazonian Craton, were individualized based on geological, petrochemical, geochronological and isotopic data (Dall'Agnol *et al.* 2005; Fig. 1): (1) Jamon suite (JS), located in the Rio Maria granite–greenstone terrain (RMGGT), represented by Jamon, Musa, Redenção, Bannach, Marajoara and Manda Saia plutons; (2) Serra dos Carajás suite (SCS) situated in the domains of the Carajás basin (CB), represented by Central, Cigano and Pojuca granites; (3) Velho Guilherme suite (VGS), occurring in the Xingu region (XR), formed by Antônio Vicente, Velho Guilherme, Mocambo, Serra da Queimada, Bom Jardim, Rio Xingu, Benedita, Ubim Norte and Ubim Sul granites (Teixeira *et al.* 2002, 2005; Lamarão *et al.* 2012).

This paper compares the morphological and compositional aspects of zircon crystals belonging to granitic bodies of the three above-mentioned suites. The data reported here were based on BSE–CL images obtained through a SEM and on semi-quantitative EDS minor element analyses. The aim is to demonstrate that these three suites can also be individualized by morphological and geochemical studies of their zircons and to highlight the efficiency of using the geochemical signature of this mineral as an indicator of tin-specialized granites and associated metals.

GEOLOGICAL CONTEXT

The three above-mentioned granite suites (Fig. 1) are located in the geochronological domain of the Central Amazonian Province (Tassinari & Macambira 2004) with the JS and SCS in Carajás Province and the VGS in the Central Amazonian Province (Santos *et al.* 2000; Vasquez *et al.* 2008). The regions represented by the CB and the RMGGT are dominated by Archean rocks (Huhn *et al.* 1988; Macambira & Lafon 1995; Souza *et al.* 2001; Leite *et al.* 2004; Dall'Agnol *et al.* 2006; Almeida *et al.* 2008; 2011; Vasquez *et al.* 2008; Oliveira *et al.* 2009a; Guimarães *et al.* 2010), which are partially hidden to the east by rocks of the Neoproterozoic Araguaia belt, whereas the XR is dominated by Paleoproterozoic volcanic and plutonic rocks with Archean Nd model ages (Teixeira *et al.* 2002; Vasquez *et al.* 2008; Juliani & Fernandes 2010). The domains of the RMGGT, CB and XR were intruded by anorogenic granites with ages ranging from 1.89 to 1.86 Ga (Tab. 1), which constitute the three investigated suites. Petrological, geochemical and isotopic studies (Dall'Agnol *et al.* 1999a, 2005; Rämö *et al.* 2002; Teixeira *et al.* 2002; Dall'Agnol & Oliveira 2007; Oliveira *et al.* 2009b) show some contrasts between these granitic suites apart from the significant differences regarding their metallogenic potential. The most important deposits of gold, iron, copper, and manganese from Carajás Province are located in the CB region. In the XR, important deposits of cassiterite and wolframite are associated with granites of the VGS. In the RMGGT, small gold occurrences associated with greenstone belts and wolframite are linked with the JS (Dall'Agnol *et al.* 2005).

PETROLOGICAL ASPECTS OF THE SUITES

The three above-mentioned suites consist of granitic batholiths and stocks (Fig. 1) emplaced at shallow crustal levels and which commonly show sharp contacts and angular enclaves, suggesting a high viscosity contrast between magmas and Archean host rocks (Dall'Agnol *et al.* 2005; Oliveira *et al.* 2009a). The rocks are isotropic, equigranular or occasionally serial, ranging from fine to coarse grained. Monzogranites with subordinate syenogranites dominate the JS. The main accessory phases of the JS are apatite, titanite, zircon, allanite, magnetite and ilmenite. Fluorite appears only in the most evolved facies (Dall'Agnol *et al.* 1999a; Oliveira *et al.* 2009a). In the SCS, the principal rocks are monzogranites and syenogranites with moderate mafic mineral contents (M < 15%). The accessory phases are similar to those of the JS, but titanite is usually absent as a primary accessory and is more common as a product of biotite alteration; fluorite and topaz are more common and tourmaline appears locally (Barros *et al.* 1995; Rios *et al.* 1995; Villas 1999). In the VGS, syenogranites are more common than monzogranites, and alkali-feldspar granites and greisens mineralized in cassiterite and wolframite occur associated with more evolved rocks. Monazite, thorite, xenotime, fluorite and columbite are also common accessories (Teixeira *et al.* 2002; Lamarão *et al.* 2012). Magnetic susceptibility (MS) data show higher values for the plutons of the JS (1.05×10^{-3} to 54.73×10^{-3}) and comparatively lower values for the dominant syenogranites of the Antônio Vicente granite of the VGS ($< 1.0 \times 10^{-3}$). The values of MS found in the SCS are more variable and generally intermediate between the former two (1.0×10^{-3} to 5.0×10^{-3}; Dall'Agnol *et al.* 2005).

Table 1. Geochronological data from Paleoproterozoic suites of the Carajás region (modified from Dall'Agnol *et al.* 2005)

Suite/Granite	Method of dating	Material	Age
Jamon			
Musa	U – Pb	Zircon	1883±5 Ma[2]
Jamon	Pb – Pb	Zircon	1885±32 Ma[3]
Redenção	Pb – Pb	Whole-rock	1870±68 Ma[4]
Serra dos Carajás			
Cigano	U – Pb	Zircon	1883±2 Ma[2]
Serra dos Carajás	U – Pb	Zircon	1880±2 Ma[2]
Pojuca	U – Pb	Zircon	1874±2 Ma[2]
Velho Guilherme			
Velho Guilherme	Pb – Pb	Whole-rock	1874±30 Ma[5]
Rio Xingu	Pb – Pb	Zircon	1866±3 Ma[6]
	Pb – Pb	Whole-rock	1906±29 Ma[6]
Mocambo	Pb – Pb	Zircon	1862±32 Ma[6]
Antonio Vicente	Pb – Pb	Zircon	1867±4 Ma[6]
	Pb – Pb	Whole-rock +kf	1896±9 Ma[6]
Bom Jardim	Pb – Pb	Zircon	1867±1 Ma[7]
Serra da Queimada	Pb – Pb	Zircon	1882±12 Ma[7]
Other Paleoproterozoic granite			
Seringa	Pb – Pb	Zircon	1895±1 Ma[1]

Data sources: (1) Paiva Júnior (2009); (2) Machado *et al.* (1991); (3) Dall'Agnol *et al.* (1999a); (4) Barbosa *et al.* (1995); (5) Macambira & Lafon (1995); (6) Teixeira *et al.* (2002); (7) Pinho (2005). kf= alkali feldspar.

According to Dall'Agnol *et al.* (2005), the three investigated suites exhibit geochemical characteristics of A-type granites, with SiO_2 contents > 65 wt.% and K_2O/Na_2O ratios typically between 1.0 and 2.0, with higher ratios towards JS – VGS – SCS. The rocks that constitute these suites are metaluminous to slightly peraluminous. Their FeOt/(MgO + FeOt) ratios are always higher than 0.80 and increase in the same direction of the K_2O/Na_2O ratios and, within the same suite, increase from the less differentiated to the more evolved varieties. The patterns of rare earth elements show moderate to pronounced negative Eu anomalies, with a particularly striking 'seagull' pattern anomaly common in the tin-granites of the VGS and leucogranites of the SCS. TDM ages of the three suites vary significantly (from 3.35 to 2.60 Ga), whereas εNd values of the JS and SCS are similar (-10.5 to -8.1 and -9.7 to -7.9, respectively) and higher than those of the VGS (-12.1 to -12.2), with the exception of the Mocambo granite (-7.9). Despite these variations, the values are consistent with derivation of the forming magmas from an Archean crustal source (Rämö *et al.* 2002).

MORPHOLOGICAL AND COMPOSITIONAL STUDY OF ZIRCONS FROM PALEOPROTEROZOIC GRANITE SUITES

Analytical procedures

Zircons from the three Paleoproterozoic granite suites were analyzed through the scanning electron microscope (LEO-1430; Geosciences Institute, Federal University of Pará, Brazil). Polished sections of selected samples were coated with carbon before BSE and EDS analyses. For CL images they were coated with gold for 30 s. Operating conditions were as follows: accelerating voltage = 20 kV, beam current = 90 μA, work distance = 15 mm, analysis time = 30 s with 4,000 – 5,000 cycles/s for each analysis. The elements analyzed were O, Si, Zr, Hf, Ce, Nb, Ta, P, Y, Th, U, Ba and Ca. A total of 3,490 analyses were performed on the rims and cores of the zircon grains, and fractures and inclusions were avoided with the aid of the BSE and CL images. Ce, P and Ba contents were consistently very low and so were excluded from Tab. 2. The analyzed zircons were selected from the Jamon and Redenção plutons of the JS; the Central, Cigano and Pojuca plutons of the SCS; and the tin-granites of the Antônio Vicente, Bom Jardim, Mocambo, Serra da Queimada and Velho Guilherme plutons of the VGS. Zircons were selected from each of the different facies of each body, from the least to the most evolved and, in some cases, from samples of the associated greisens.

RESULTS

Table 2 presents the average chemical composition from zircon crystals of granites and associated greisens. A total of 3,490 EDS analyses were performed, including 571 zircon analyses from the JS, 1,565 from the SCS and 1,354 from the VGS.

JAMON SUITE

Jamon and Redenção granites have predominantly subhedral to euhedral zoned zircons, which are locally fractured and free of corrosion. Inclusions of apatite are common (Fig. 2). The mean contents of Hf are relatively low and show little variability (1.9 -2.3 wt.%), even in the leucogranites of the Redenção pluton (2.2 wt.%), producing Zr/Hf ratios between 24 and 29 (Tab. 2). The average contents of Y are lower than 1.0 wt.%, except for the zircons of Redenção leucogranite, which presented a mean Y content of 1.5 wt.%, producing Zr/Y ratios between 64 and 81 for the first case and that of approximately 56 for the second. The Nb content in these zircons has a mean value of 1.2 and 0.2 wt.% to Th and U, respectively. The sum of Hf + Y + Th + U ranged from 4.2 and 3.0 wt.%, with the Redenção leucogranite presenting higher average contents (Tab. 2).

SERRA DOS CARAJÁS SUITE

Zircons of the SCS from Central, Cigano and Pojuca granites are morphologically and compositionally distinct from those of the JS (Fig. 3, Tab. 2). Subhedral to anhedral crystals dominate and are often fractured and corroded, assuming sieve aspect. Alterations in the form of irregular patches, usually with high Ca contents, and thorite inclusions are observed in many crystals (Fig. 3). Anhedral crystals of thorite (≤50 μm) associated with zircons are common in greisens of the Cigano granite (Fig. 3F). Compositionally, zircons of the SCS showed average Hf contents (3.1 wt.%) higher than those of the JS (2.1 wt.%), resulting in comparatively lower Zr/Hf average ratios (19.0 for the JS and 26.0 for the SCS). Zircons from biotite monzogranite, biotite leucogranite and syenogranite of the Pojuca pluton showed the highest concentrations of Hf (2.7 – 5.8 wt.%) and the lowest Zr/Hf ratios (20.5 to 7.6). With the exception of the leucogranite of the Redenção pluton, the Y contents in the zircons of the SCS are generally slightly higher than those of the JS (averaging 1.1 wt.% in the SCS and 0.9 wt.% in the JS). However, higher contents of this element were found in zircons from Pojuca leucogranites (1.6 wt.%), yielding a Zr/Y average ratio lower than that of the rocks of the JS (63.0 *versus* 70.0 wt.%). The contents of U and Th are also slightly higher in the zircons from the SCS, yielding values of Hf + Y + U + Th between 3.5 and 8.6 wt.% (Tab. 2), which is generally higher than the maximum value obtained from zircons of the JS (4.2 wt.%).

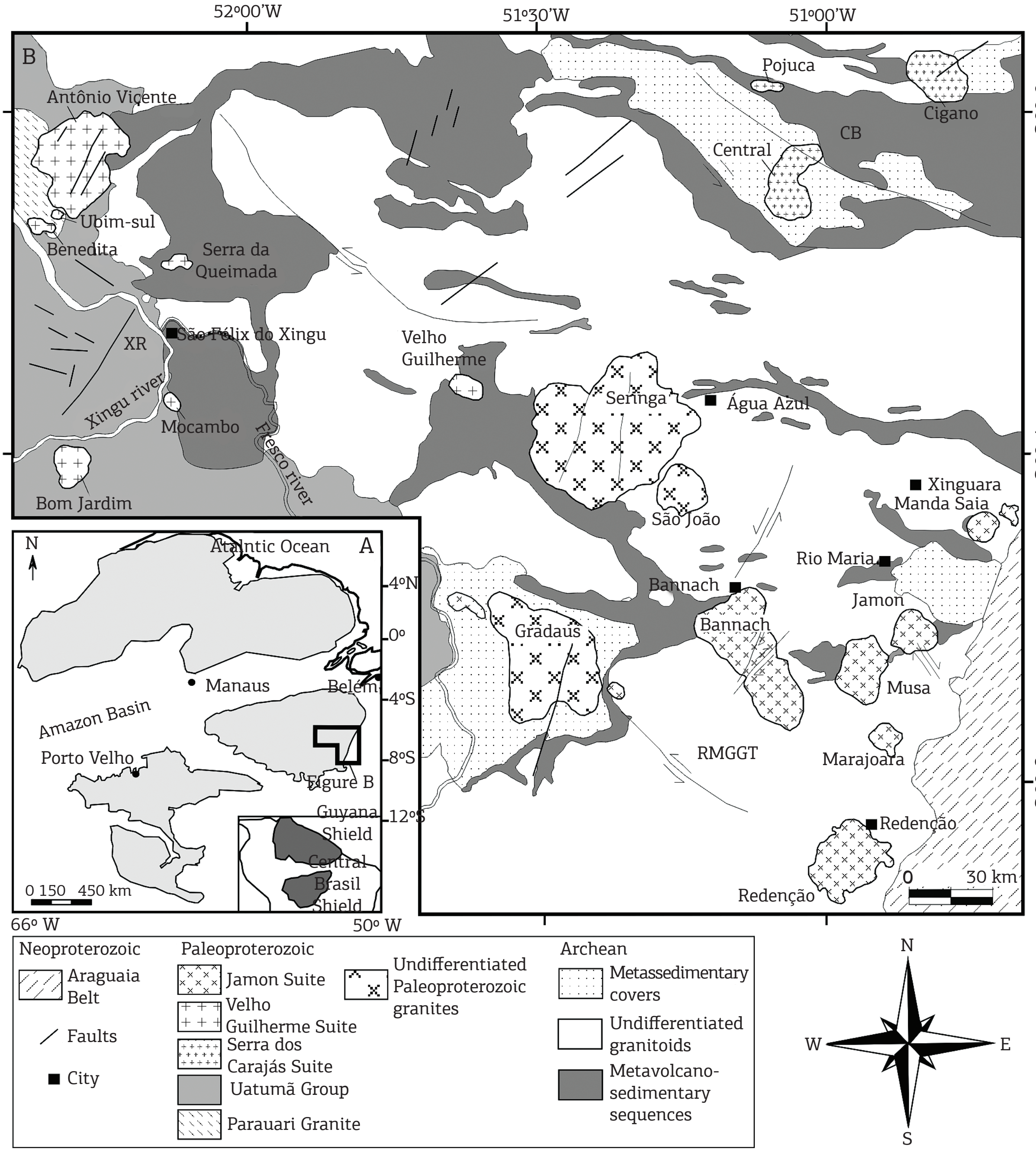

RMGGT: Rio Maria granite–greenstone terrain; CB: Carajás basin; XR: Xingu region.

Figure 1. Simplified geological map of the Carajás Province showing the distribution of A-type granites that comprise the Paleoproterozoic granite suites. (modified from Dall'Agnol *et al.* 2005).

VELHO GUILHERME SUITE

Zircons of the VGS show subhedral shapes in the less evolved rocks, becoming dominantly anhedral and rounded in the most evolved and associated greisens (Figs. 4 and 5). In the latter, the zircons are strongly corroded, with dark Ca-enriched patches and frequent inclusions of minerals of Th, U and REE, indicating that the crystals were affected by hydrothermal processes responsible for formation of these rocks. In syenogranite rocks and greisens of the Bom Jardim granite, the zircons are associated with anhedral crystals of cassiterite and columbite (Fig. 4F), and show great morphological similarity with those of the evolved rocks and greisens of the SCS (Fig. 3). Compositionally, zircons of the VGS have Hf contents higher than 2.5 wt.%, with the exception of zircons from the less evolved rocks (BASMG and BMG) of the Antônio Vicente granite (1.9 and 2.2 wt.%, respectively) and zircons from the heterogranular syenogranite rocks of

Table 2. The average chemical analysis (wt.%) of investigated zircon grains performed by EDS

Suite/ Granite	Facies	Sample	O	Si	Ca	Y	Zr	Nb	Hf	Ta	Th	U	Zr/ Hf	Zr/Y	Σ
JAMON															
Jamon (249)	ABMG	AU-390 (74)	26.2	13.1	0.1	0.7	53.8	1.2	2.0	0.8	0.2	0.2	27.9	78.6	3.1
	BMGH	AU-375 (126)	26.2	13.2	0.1	0.8	53.7	1.2	1.9	0.8	0.2	0.2	28.6	76.1	3.0
	BMG	AU-382 (49)	27.3	13.1	0.5	0.8	51.7	1.2	2.3	0.8	0.2	0.2	23.6	81.2	3.6
Redenção (322)	ABMG	DCR-36B (124)	24.9	13.2	0.1	0.9	54.4	1.1	2.1	1.0	0.2	0.2	26.8	64.0	3.4
	BMG	DCR-33B (98)	26.9	13.2	0.3	0.8	52.4	1.2	2.3	0.8	0.2	0.2	24.0	66.0	3.6
	Leucogr.	DCR-83B (100)	26.4	13.1	0.5	1.5	51.8	1.1	2.2	1.0	0.2	0.3	24.7	56.5	4.2
		Average	26.3	13.1	0.3	0.9	53.0	1.2	2.1	0.9	0.2	0.2	25.9	70.4	3.5
SERRA DOS CARAJÁS															
Central (462)	ABMG	GF1-26,7 (171)	28.1	13.0	0.6	0.8	51.3	1.1	2.2	0.8	0.2	0.3	24.5	67.5	3.5
	ABMG	CRD-01 (123)	28.9	12.7	1.1	1.2	49.6	1.1	2.2	0.8	0.1	0.5	23.3	60.2	4.0
	ABSG	CRD-04 (65)	30.0	12.7	1.3	1.0	47.7	1.0	2.7	0.9	0.2	0.5	19.0	60.0	4.4
	BSG	MR-158 (103)	28.3	12.7	0.7	1.2	48.4	1.0	3.9	0.8	0.1	0.8	15.9	56.3	6.0
Cigano (550)	ABMGP	34-A (85)	27.0	13.3	1.5	1.1	50.1	1.1	2.1	0.9	0.3	0.5	24.5	55.1	4.0
	BMG	ECR-91B (131)	24.6	13.3	0.4	0.8	54.1	1.2	2.2	0.9	0.3	0.3	25.8	75.5	3.6
	BMSG	96 (120)	24.1	13.4	0.7	1.0	53.8	1.2	2.2	0.9	0.3	0.4	25.4	63.5	3.9
	Greisen	CIG-5 (214)	23.6	12.8	0.4	0.9	55.6	1.8	2.6	0.8	0.2	0.3	22.8	62.3	4.0
Pojuca (553)	ABMG	F-11 (117)	26.9	13.0	0.9	0.8	51.9	1.2	2.6	0.8	0.2	0.4	21.7	76.2	4.0
	BMG	F-33 (131)	26.7	11.8	1.5	0.9	43.7	0.9	3.7	0.6	0.3	0.6	12.1	59.3	5.5
	BMSG	F-6 (153)	29.4	12.7	1.5	1.1	47.5	1.4	2.7	1.0	0.4	0.4	20.5	65.6	4.6
	Leucogr.	F-30 (72)	30.2	12.9	1.5	1.6	43.6	0.9	5.5	0.6	0.7	0.8	8.1	50.3	8.6
	Hydr. L.	F-36 (80)	28.6	12.6	1.0	1.6	44.7	1.0	5.8	0.6	0.4	0.6	7.6	66.4	8.4
		Average	27.4	12.8	1.0	1.1	49.4	1.2	3.1	0.8	0.3	0.5	19.3	62.9	5.0

Continue...

Table 2. Continuation

Suite/ Granite	Facies	Sample	O	Si	Ca	Y	Zr	Nb	Hf	Ta	Th	U	Zr/ Hf	Zr/Y	Σ
VELHO GUILHERME															
Antonio Vicente (450)	BASMG	IE-02 (76)	27.6	12.7	0.2	0.8	52.1	1.6	1.9	0.9	0.2	0.2	29.6	70.1	3.1
	BMG	GAMCS54 (38)	28.9	12.3	0.6	1.2	49.9	1.0	2.2	1.0	0.3	0.4	23.1	55.7	4.1
	BSGA	AVBA4 (96)	27.4	12.6	0.9	0.9	51.2	0.9	2.6	1.0	0.2	0.5	22.0	62.4	4.2
	BSGIA	NEB75 (70)	29.8	12.3	0.9	1.4	47.8	0.9	2.9	0.9	0.2	0.8	18.1	58.5	5.3
	Greisen 1	AVIN10 (92)	27.9	11.5	0.5	2.5	48.5	1.1	3.2	0.9	0.9	0.5	17.2	59.5	7.1
	Greisen 2	NRAV26B (78)	28.5	12.6	0.4	1.1	50.4	1.2	2.5	0.8	0.1	0.4	21.9	56.4	4.1
Bom Jardim (439)	BMG	SAL72 (123)	33.3	11.5	0.6	6.4	38.5	0.8	3.7	0.7	0.5	1.1	11.7	17.4	11.7
	BMG	SAL29 (114)	31.7	11.7	0.3	1.2	45.2	0.9	3.9	0.7	1.5	0.8	13.1	55.9	7.4
	BSG	SAL-49 (81)	30.2	11.8	1.3	1.7	44.0	1.3	5.4	0.7	0.4	1.0	8.5	51.6	8.5
	Greisen 1	SAL-100 (79)	31.4	11.3	0.5	1.5	45.8	0.7	3.4	0.9	0.7	1.6	14.2	52.9	7.2
	Greisen 2	SAL-66b (42)	30.6	9.9	0.8	3.5	39.3	0.8	5.8	0.8	3.3	2.5	7.0	20.6	15.1
Mocambo (200)	PSMG	GM-56A (55)	23.3	11.7	0.5	1.5	53.1	0.6	3.7	2.4	0.4	1.2	15.2	61.4	6.8
	PSMG	GM-17B (68)	24.8	11.7	0.7	2.1	50.7	0.6	4.0	2.1	0.6	0.9	14.5	53.3	7.6
	Greisen	GM-23A (77)	24.6	12.4	0.6	1.3	52.8	0.7	3.1	1.9	0.2	0.6	17.5	52.0	5.2
Serra da Queimada (161)	BMG	SQ22 (71)	26.1	11.7	1.1	3.1	48.7	1.7	3.0	0.9	0.9	1.1	17.0	34.4	8.1
	BSG	SQ11 (90)	27.4	12.1	1.0	2.2	48.3	1.5	3.5	0.8	0.4	1.0	15.0	35.6	7.1
Velho Guilherme (104)	HSG	NNVG-38 (58)	25.6	12.9	0.2	0.9	53.9	1.0	2.1	1.1	0.2	0.2	26.9	64.7	3.4
	ESG	NNVG-31 (46)	31.4	12.1	1.0	5.4	41.7	0.8	2.8	1.3	0.7	0.5	16.3	26.6	9.4
Total of analysis = 3,490		Average	28.4	11.9	0.7	2.2	47.9	1.0	3.3	1.1	0.6	0.8	17.2	49.4	7.0

ABMG: amphibole-biotite monzogranite; HBMG: heterogranular biotite monzogranite; BMG: biotite monzogranite; PABMG: porphyritic amphibole-biotite monzogranite; BMSG: biotite monzogranito to syenogranite; BASMG: biotite-amphibole syenogranite to monzogranite; PSMG: porphyritic syenogranite to monzogranite; HSG: heterogranular syenogranite; ESG: equigranular syenogranite; Leucogr.: leucogranite; Hydr. L.: hydrothermalized leucogranite; A: altered; I: intensely. Σ: sum Hf + Y + Th + U (ppm). Number of analyses in parentheses.

the Velho Guilherme pluton (2.1 wt.%). Zircon crystals of the monzogranites rocks of the Mocambo and Bom Jardim granites and greisens associated with the Antônio Vicente granite have clearer and intensely corroded rims surrounding more preserved and, it seems, older cores (Figs. 4D and 4E and 5A). In the zircons of the Bom Jardim granite, such rims include contents of up to 3.9 wt.% Hf, 5.1 wt.% Th and 1.8 wt.% U, whereas the cores showed concentrations of 2.9 wt.% Hf and 0.5 wt.% for both Th and U. In the Mocambo granite, the Hf contents in the edges of some crystals reached 5.0 wt.% (Fig. 5A). In the greisens of the Antônio Vicente granite, the Hf contents in the rim zone of the zircons reached 5.9 wt.%; however, the contents of Th and U did not exceed 1.0 wt.% (Fig. 4D).

Zircons of the VGS showed a mean Hf content of 3.3 wt.% and the lowest Zr/Hf mean ratio (17.2) among the three suites. Y, Th and U show average grades (2.2, 0.6 and 0.8 wt.%, respectively), slightly higher than those of the zircons from the other two suites and yielding average Zr/Y ratios comparatively lower (49.4, Tab. 2) than the other two suites. Hf + Y + U + Th of the VGS zircons vary from 3.1 wt.% in amphibole monzogranites of the Antônio Vicente granite to 15.1 wt.% in greisens of the Bom Jardim pluton, with an average value of 7.0 wt.%. The average content of Nb and Ta is 1.0 and 1.1 wt.%, slightly lower and higher, respectively, compared with the contents in zircons of the other two granitic suites.

DISCUSSION

Zircon as an indicator of specialized granites

Systematic studies on the geochemical signature of zircon, reflected in the abundance of certain trace elements, especially Hf, indicate that zircon can be used as a geochemical tracer. Such data may be useful in identifying the nature of their source rocks and crystallization environment, in the characterization of magmatic fractionation processes and in provenance studies of detrital zircons (Heaman *et al.* 1990; Uher *et al.* 1998; Hoskin & Ireland 2000; Pupin 2000; Wang *et al.* 2000; Belousova & Grifffin 2002). This is because Zr and Hf have similar ionic radii and electrical charges. Because most of the Zr and Hf contents in granitic rocks are incorporated into zircon crystals, the Zr/Hf ratio of this mineral can be considered to approximate the Zr/Hf ratio of the source magma (Owen 1987). Wang *et al.* (1996) concluded that Hf-rich zircons from S-type granites of Suzhou (China) have formed as a result of fractional crystallization processes, which would indicate the tendency of enrichment in that element during magmatic differentiation. Zircons of peralkaline granites of Laoshan complex, China, also have Hf-enriched edges, but the same rocks were interpreted by Wang *et al.* (1996) as resulting from hydrothermal activities. Wang *et al.* (2000) assumed that zircons from granitic rocks with high levels of Hf are typical of evolved granites also enriched in rare metals (Sn, Mo, Ta, W, Li), and high-Hf zircon occurrence would mark the passage from granite to pegmatites with rare metals. Kempe *et al.* (2004) demonstrated that granites with topaz and rare metals have extremely low Zr/Hf ratios, interpreted as a primary signature of evolved granitic liquids or, alternatively, as a signature produced during processes of albitization of the host rocks by F-enriched fluids. Lamarão *et al.* (2007, 2010, 2012) performed compositional and textural studies of zircons by SEM-EDS from granites and associated greisens from tin provinces of southern Pará, Pitinga and Rondônia, and compared the data with those provided by zircons from granites without tin in the south-eastern Amazon Craton. The zircons from tin granites showed Hf enrichment and lower Zr/Hf ratios than those of granites without tin, indicating that a geochemical signature of zircon can be used, even through semi-quantitative EDS analysis, as a preliminary indicator of specialized granites.

Composition of zircons and the metallogenic potential of the studied granitic suites

Zircons from tin granites of the VGS are predominantly anhedral, altered and corroded, especially in the more evolved rocks and associated greisens (Figs. 4 and 5). Compositionally, they are more enriched in Hf, Y, Th and U, have lower Zr/Hf and Zr/Y ratios and the highest values of Hf + Y + U + Th compared with zircons of the other two suites (Tab. 1). In general, these elements tend to increase in the more evolved rocks (*e.g.*, in the Antônio Vicente and Bom Jardim granites), suggesting that magmatic differentiation plays an important role in this enrichment (Wang *et al.* 1996, 2000). In some cases, zircons of greisens associated with these granites have concentrations of these elements that are similar or higher than those of zircons from magmatic facies formed during the magmatic stage (*e.g.*, greisens of the Antônio Vicente and Bom Jardim granites). Furthermore, some zircons have overgrowth edges that are heavily corroded and enriched in Hf, Y, Th and U relative to their cores (Figs. 4E and 5A), suggesting that tardi-magmatic fluids may have caused textural changes as well as enrichment in these trace elements in the early zircons (Wang *et al.* 1996). Textural features resulting from overgrowth may also have developed in sub-solidus conditions during the stage of greisenization, as found in zircons from greisens associated with the Antônio Vicente pluton (Fig. 4D).

In the SCS, the Pojuca granite (Horbe 1998) has zircons with morphological and compositional characteristics closer to those of zircons from tin granites of the VGS (Fig. 3, Tab. 2). The high content of Hf and the low Zr/Hf ratios present, especially in zircons from leucogranites,

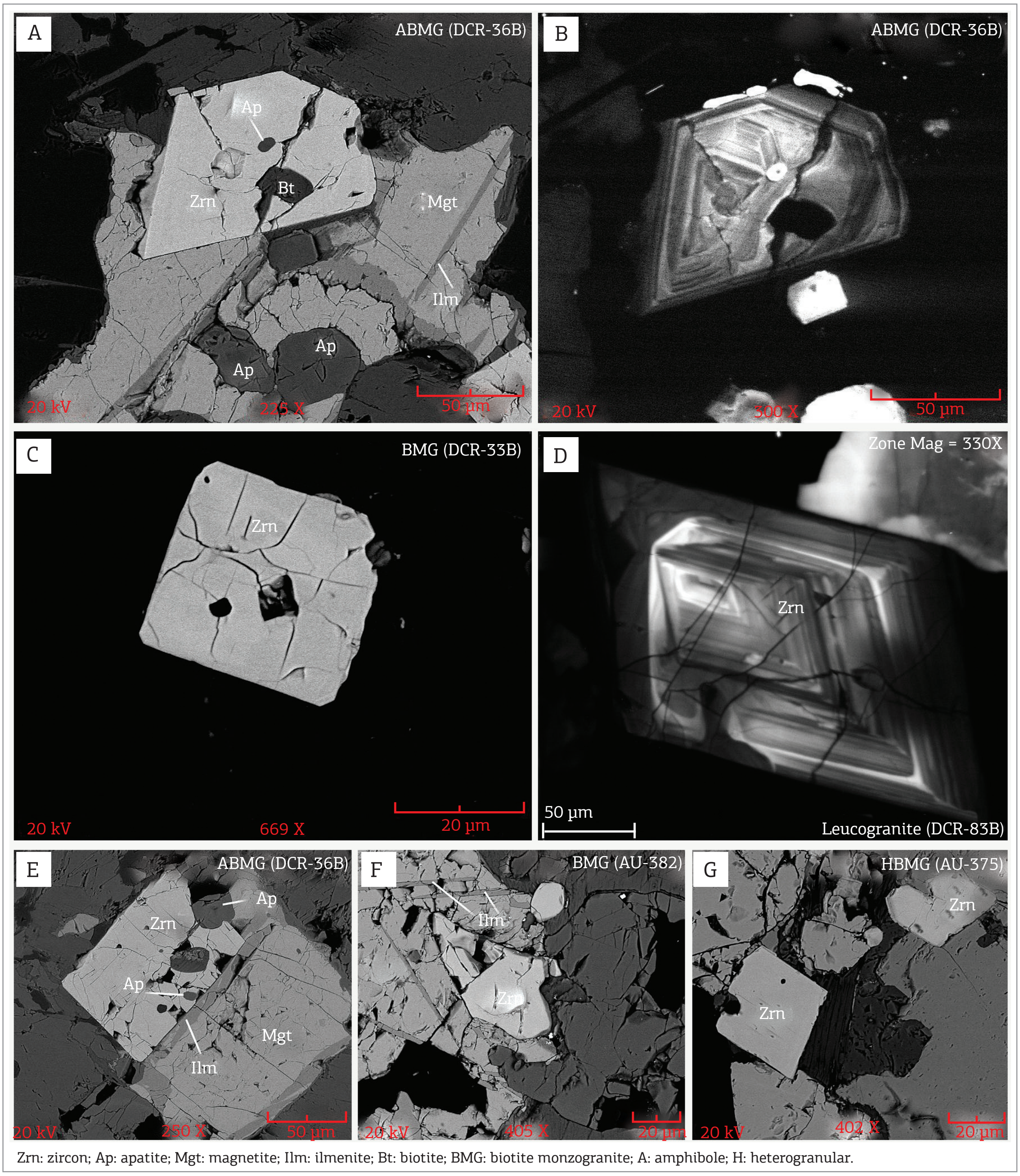

Zrn: zircon; Ap: apatite; Mgt: magnetite; Ilm: ilmenite; Bt: biotite; BMG: biotite monzogranite; A: amphibole; H: heterogranular.

Figure 2. Images of backscattered electron (A, C, E, F and G) and cathodoluminescence (B and D) of zircons from the Redenção (A–D) and Jamon (E–G) granites.

suggest that the more evolved varieties of the Pojuca pluton have the potential to generate tin mineralization. However, even in these more evolved rocks, the SEM analyses found no presence of cassiterite, suggesting that factors other than composition can lead to the development of tin mineralization. In Central granites, despite the intense alteration and corrosion present in zircons (Figs. 3A to 3C), the levels of Hf and Y are, except in the syenogranites, lower and have Zr/Hf and Zr/Y ratios higher than those of the typical tin granites of the VGS (Tab. 2). Rios *et al.* (1995) and Barros *et al.* (1995) performed petrographic and metallogenic evaluation of the potential in the northern and western portions, respectively, of the Central granite and did not identify any evidence of magmatic or hydrothermal tin mineralization,

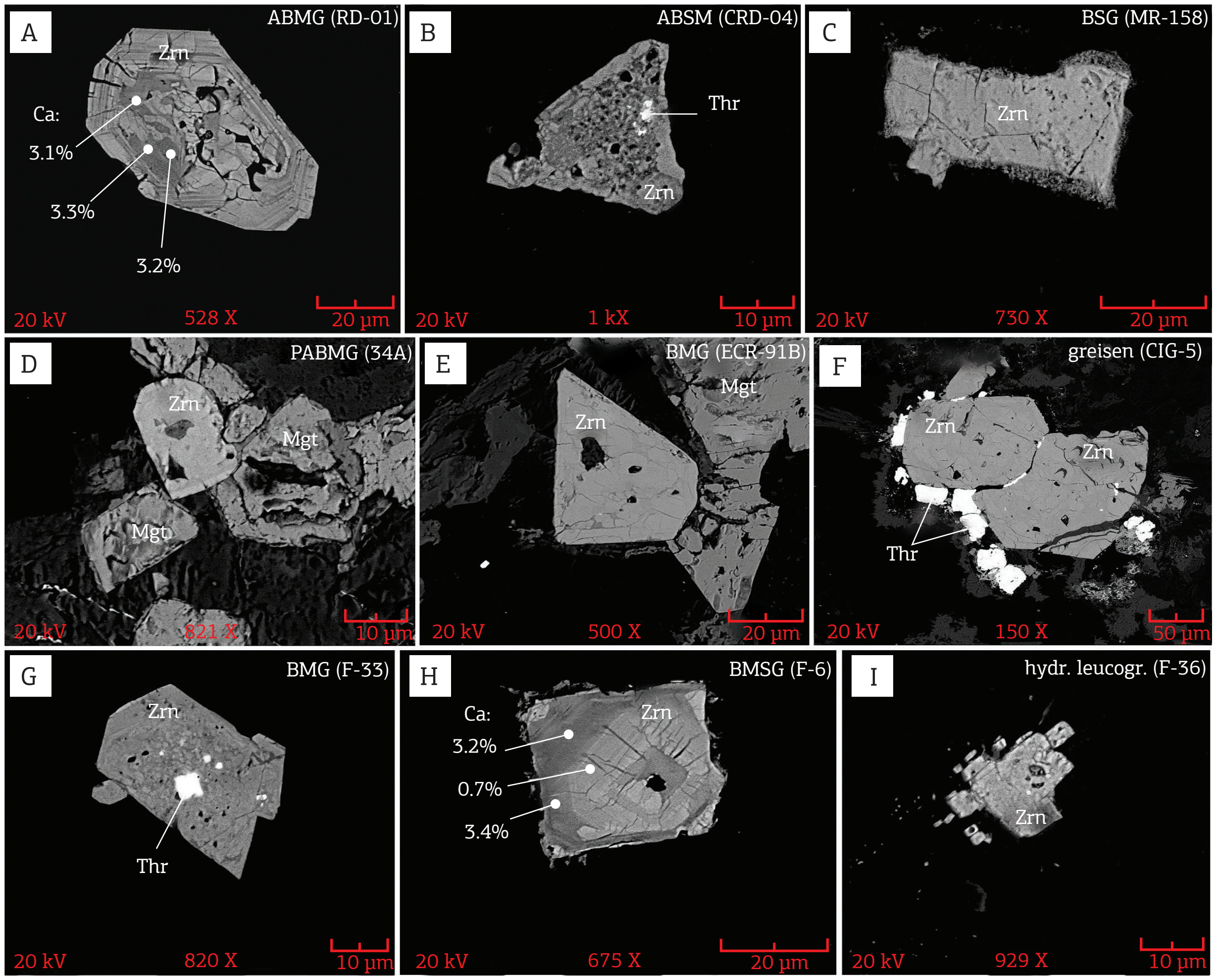

Zrn: zircon; Thr: thorite; Mgt: magnetite; BMG: biotite monzogranite; A: amphibole; P: porphyritic; S: syenogranite; hydr. leucogr.: hydrothermal leucogranite.

Figure 3. Backscattered electron images of zircons from the Central (A – C), Cigano (D – F) and Pojuca (G – I) granites of the Serra dos Carajás suite. (A) Altered, fractured and corroded euhedral crystal; dark patches with high contents of Ca; (B) Anhedral crystal intensely corroded showing sieve texture and fine thorite inclusions; (C) Fractured and corroded anhedral crystal; (D – F) Altered and fractured subhedral crystals associated with magnetite and thorite crystals; (G) Subhedral and corroded crystal, displaying sieve aspect on the central portion and fine thorite inclusions; (H) Compositionally zoned and fractured crystal, showing Ca-enriched dark zones in relation to light zone; (I) Thin zircon crystal intensely altered.

such as albite granites, greisens or rocks containing siderophyllite and/or topaz. The petrographic and geochemical characteristics observed contrast with the granites specialized in Sn. Greisens associated with Cigano granite have zircons with the Zr/Hf ratios very similar (~ 23) to those found in zircons from monzogranite and syenogranite rocks (24 – 26) and were also not identified as having Sn mineralization in this body, indicating that the geochemical signature of magmatic zircons was most likely preserved during the stage of greisenization of the pluton.

In turn, Redenção and Jamon granites have well-developed zircons that are predominantly euhedral to subhedral, contain frequent inclusions of apatite (Fig. 2), are depleted in Hf and have Zr/Hf ratios much higher than those of zircons from the other two suites (Tab. 2), which are all geochemical characteristics in agreement with their low potential for generating tin deposits. However, there are occurrences of wolframite in the Pedra Preta deposit at western edge of Musa granite (not investigated here). W can be associated with different types of granites and has little dependence on the oxidation state of the magma (Blevin & Chappell 1992, 1995; Blevin *et al.* 1996). In the Pedra Preta deposit, the data suggest a metamorphic origin for the mineralizing solutions, although the Musa granite is an alternative for the origin of W (Rios *et al.* 2003). Figure 6 shows the variation of the Zr/Hf ratios in zircons of the studied granites and indicates the associated mineralization with the same, whereas Fig. 7 compares these ratios to the contents of Hf + Y + U + Th obtained by SEM-EDS.

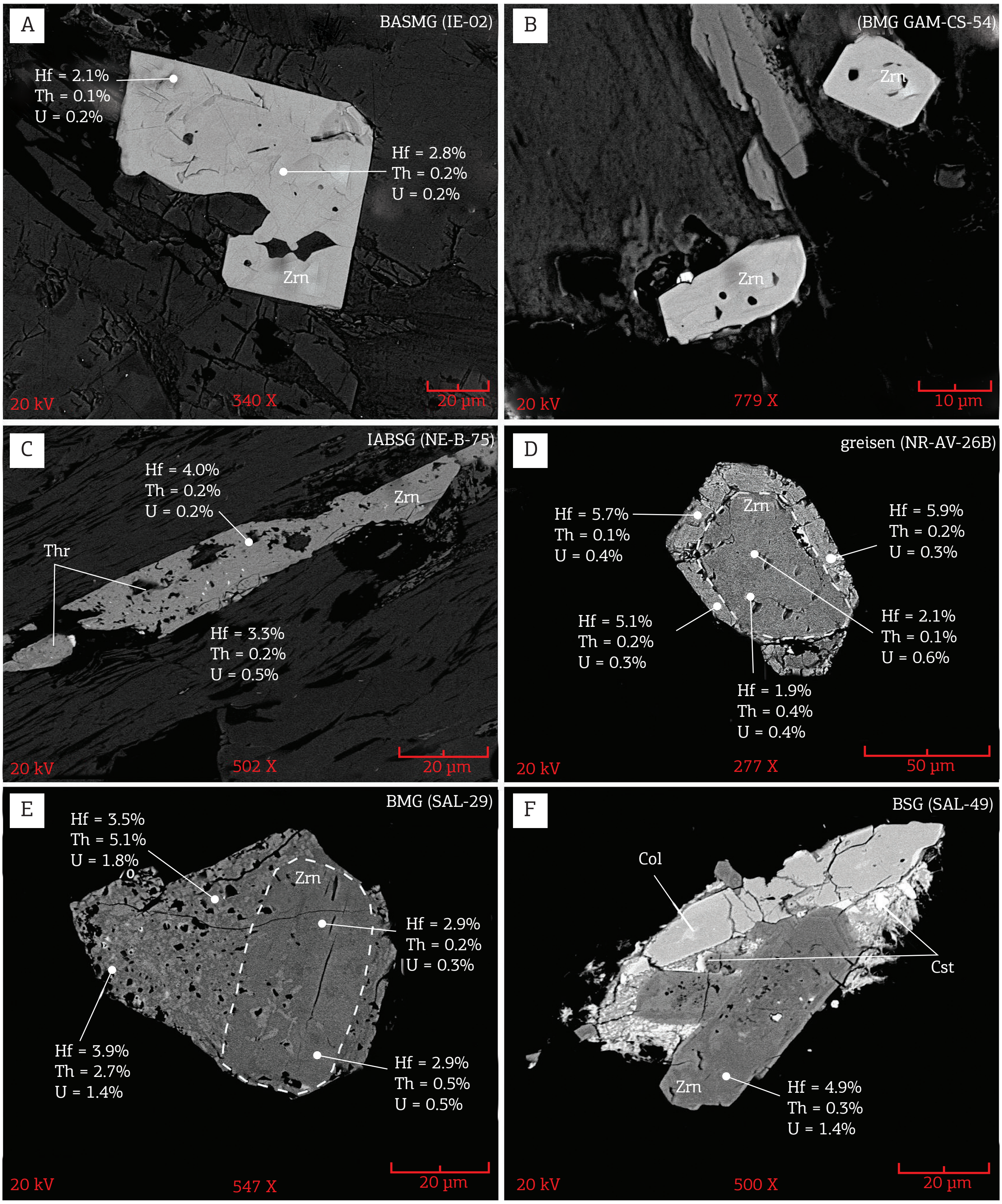

BASMG: biotite-amphibole syenogranite to monzogranite; BMG: biotite monzogranite; BSG: biotite syenogranite; IA: intensely altered; Zrn: zircon; Thr: thorite; Cst: cassiterite; Col: columbite.

Figure 4. Backscattered electron images with EDS analyses of zircons from Antonio Vicente (A – D) and Bom Jardim (E and F) granites, Velho Guilherme suite. (A and B) Subhedral and slightly altered crystals of less evolved facies (BASMG and BMG), with comparatively lower contents of Hf, Th and U; (C) Subhedral and corroded crystals containing inclusions of thorite and higher contents of Hf, Th and U; (D) Subhedral crystal slightly altered showing Hf-enriched overgrowth mantle in relation to its core; (E) Crystal with more homogeneous subhedral core and mantle heavily corroded. Note higher contents of Hf, Th and U in the latter. Subhedral zircon crystals with high contents of Hf and U, associated with crystals of tin and columbite.

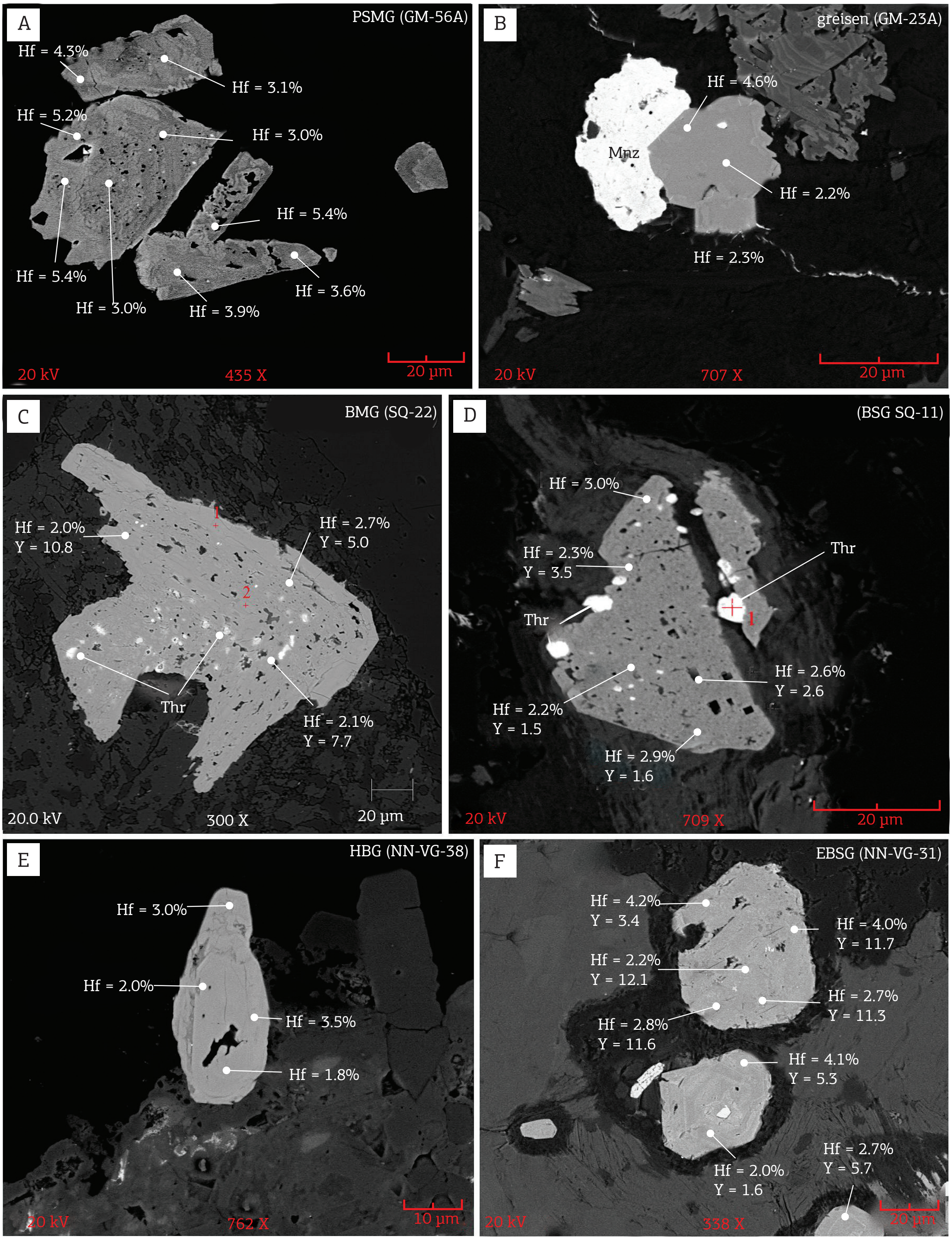

E: equigranular; H: heterogranular; BMG: biotite monzogranite; BSG: biotite syenogranite; PSMG: porphyritic syenogranite to monzogranite.

Figure 5. Backscattered electron images with EDS analyses of zircons from Mocambo (A and B), Serra da Queimada (C and D) and Velho Guilherme (E and F) granites, Velho Guilherme suite. (A) Altered and corroded crystals with Hf-enriched edges; (B) Anhedral crystals with higher Hf content at the edges associated to monazite crystals; (C and D) Anhedral and heavily corroded crystals, resembling to sieve with fine inclusions of thorite (Thr) and high concentrations of Y; (E and F) Subhedral to anhedral altered and corroded crystals showing variable concentrations of Hf and Y.

A frequency histogram with the Zr/Hf ratios of the studied zircons (Fig. 8) shows that the zircons from granites of the VGS have the Zr/Hf ratios comparatively lower than those of the JS, with a mode of 15 for the VGS and 25 for the JS. The zircons from plutons belonging to the SCS have Zr/Hf ratios that span the range of values found in zircons of the VGS and JS, but the mode found for the ratios of zircons from the SCS was 22. The zircons from evolved rocks of the Pojuca and Central granites are responsible for the lower values of this ratio. The VGS samples mineralized in cassiterite, wolframite and columbite have zircon crystals with the Zr/Hf ratios between 5 and 22 (Figs. 6 to 8).

Composition of Zircons and Magmatic Series

MS, mineral chemistry and experimental studies (Dall'Agnol *et al.* 1999b, 2005; Dall'Agnol & Oliveira 2007; Oliveira *et al.* 2009b) demonstrate that the granites of the JS formed under predominantly oxidizing conditions (coincident or slightly higher than the buffer nickel/nickel oxide (NNO), whereas the dominant syenogranites of the VGS (Teixeira *et al.* 2002) evolved under reducing conditions (lower than the fayalite-magnetite-quartz – FMQ – buffer), fitting, respectively, in magnetite and ilmenite series of Ishihara (1981). In the SCS, the dominant Fe – Ti oxide mineral is magnetite, suggesting that these rocks were formed under oxidizing conditions. However, there is an apparent contradiction because the Fe/(Fe + Mg) ratios obtained in whole rock, amphibole and biotite are very high and compatible with those of reduced granites (Dall'Agnol *et al.* 2005; Dall'Agnol & Oliveira 2007). For this reason, the authors conclude that the granites of the SCS formed in moderately reduced conditions, situated above the FMQ buffer, to justify the presence of magnetite, but near the buffer to explain the high Fe/(Fe + Mg) ratios. Sn mineralization is commonly associated with reduced granites of ilmenite series (Ishihara 1980). These may be accompanied by W and Ta mineralization, but there are also W-mineralized granites formed under oxidizing conditions (Blevin & Chappell 1992, 1995; Blevin *et al.* 1996). This would explain the occurrence of this type of mineralization associated with bodies of the JS.

In this context, the zircon compositional data obtained in this study corroborate the characterization of the metallogenetic potential of the three suites from Carajás Province, as demonstrated by the occurrence of hydrothermal mineralization of

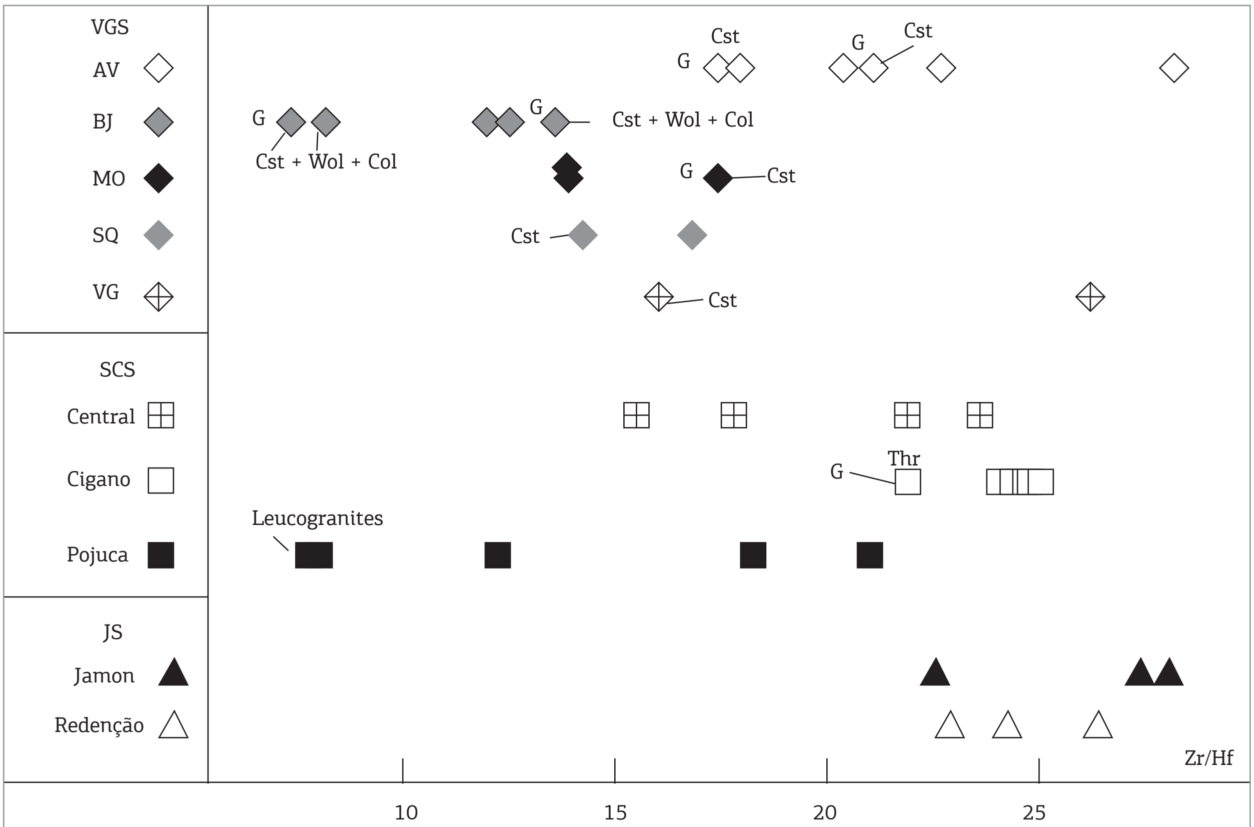

VG: Velho Guilherme; SQ: Serra da Queimada; MO: Mocambo; BJ: Bom Jardim; AV: Antonio Vicente; G: greisen; Cst: cassiterite; Wol: wolframite; Col: columbite; Thr: thorite.

Figure 6. Distribution of Zr/Hf means ratios of zircons from magmatic and hydrothermal facies associated with each of the plutons of the studied suites: Jamon suite (JS), Serra dos Carajás suite (SCS) and Velho Guilherme suite (VGS).

Sn associated with reduced rocks of the VGS, and its absence in granites of the oxidized JS. The SCS is located in intermediate conditions in relation to the other two suites in terms of oxygen fugacity (Dall'Agnol *et al.* 2005; Dall'Agnol & Oliveira 2007) and shows morphological and compositional variations of zircons similar to the tin granites of the VGS. Although no Sn mineralization associated with this suite has been identified, occurrences of anomalies of tin were detected at the north-west edge of the Central granite (Barros *et al.* 1995). This indicates that although this suite is not the most favorable for tin mineralization, its characteristics are not entirely incompatible with those of specialized granites. Therefore, tin mineralization could occur associated with their more evolved facies, but would likely be of small volume and less expressive than the mineralization associated with the VGS.

CONCLUSIONS

Zircons of the three granitic suites show remarkable compositional and morphological differences. In the JS, they form euhedral to subhedral well-developed crystals, without evident alteration and corrosion. In terms of composition, they have low contents of Hf, Y, Th and U; their higher Zr/Hf ratios, even in its most evolved rocks (leucogranites of the Redenção granite), indicate a very low potential for the generation of Sn deposits compared to zircons from the granites of the other two studied suites. Zircons from tin granites of the VGS are subhedral in the less evolved rocks (BASMG) to dominantly anhedral, altered and strongly corroded, Hf enriched and have Zr/Hf ratios that decrease towards the more evolved rocks and associated greisens. The greisens mineralized in Sn, W and Ta of this suite contain zircons with the Zr/Hf ratios between 5 and 22, indicating that zircons from reduced granites with the Zr/Hf ratios of this order may be used in preliminary prospective studies of specialized granite bodies. Zircons from the SCS showed medium contents of Hf + Y + Th + U and Zr/Hf ratios intermediate between those found in the zircons of the JS and VGS (Tab. 2). However, in the frequency histogram constructed from the total number of analyses performed in this study, the Zr/Hf ratios of zircons from the SCS encompass the range of values yielded by the zircons of the JS and VGS. Although zircons of the Pojuca granite are morphologically and geochemically similar to those of the VGS, there were no observed occurrences of tin mineralization in its rocks. The occurrence of tin anomalies in stream sediments near the north-western edge of the Central granite of the SCS (Barros *et al.* 1995) indicates that the more evolved varieties of this suite can generate such mineralization. This can be explained by the moderately reducing character of its magma, which, though less favorable than in the case of the granites of the VGS, is not incompatible with generating the tin mineralization associated with their more evolved facies.

Greisens associated with Cigano granite do not have tin mineralization. The zircons found in these greisens have an average Zr/Hf ratio that is similar to that of the host granite. Similar to observations in the Pitinga Province, the processes of greisenization apparently preserved the geochemical signature of the magmatic zircons. Zircon crystals found in greisens are generally remnants of the host granite.

This study showed the importance of the morphological features and geochemical signature of zircons, reflected mainly in their Hf contents and Zr/Hf ratios, on

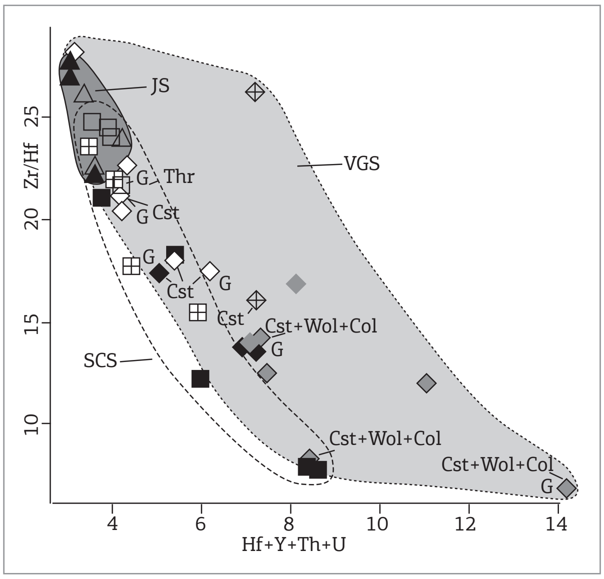

Figure 7. Zr/Hf *versus* Hf + Y + U + Th diagram (wt.%) of zircons from granites of the Jamon suite (JS), Serra dos Carajás suite (SCS) and Velho Guilherme suite (VGS). Symbols and abbreviations as in Fig. 6.

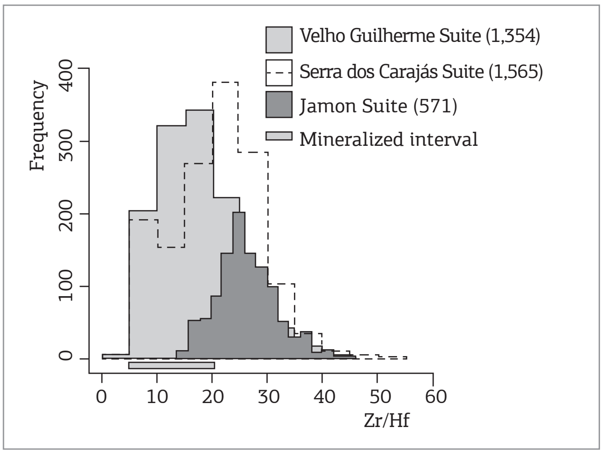

Figure 8. Frequency histogram showing Zr/Hf ratios of zircons from granites of the Jamon, Serra dos Carajás and Velho Guilherme suites. Number of EDS analyses in parentheses.

the identification of specialized tin granites. The chemical differences presented by the zircons of the three studied granitic suites corroborate the petrological, geochemical, and MS characteristics, allowing their individualization. Analysis of zircon by SEM-EDS can therefore be used in the preliminary evaluation of the granite metallogenetic potential for Sn mineralization and likely other metals.

ACKNOWLEDGMENTS

Geosciences Institute of UFPA and colleagues of the Group of Research on Granite Petrology of the UFPA. This paper is a contribution to the Amazonian Institute of Geosciences – GEOCIAM, Program (INCT – CNPq/MCT/FAPESPA – Proc. 573733/2008-2).

REFERENCES

Almeida J.A.C., Dall'Agnol R., Oliveira M.A., Macambira M.J.B., Pimentel M.M., Rämö O.T., Guimarães F.V., Leite A.A.S. 2011. Zircon geochronology and geochemistry of the TTG suites of the Rio Maria Granite-Greenstone terrain: Implications for the growth of the Archean crust of the Carajás Province, Brazil. *Precambrian Research*, **187**:201-221.

Almeida J.A.C., Oliveira M.A., Dall'Agnol R., Althoff F.J., Borges R.M.K. 2008. *Relatório de mapeamento geológico na escala 1:100.000 da Folha Marajoara (SB-22-Z-C-V)*. Programa Geobrasil, CPRM - Serviço Geológico do Brasil, 147 p.

Barbosa A.A., Lafon J.M., Neves A.P., Vale A.G. 1995. Geocronologia Rb-Sr e Pb-Pb do Granito Redenção, SE do Pará: Implicações para a evolução do magmatismo proterozóico da região de Redenção. *Boletim do Museu Paraense Emílio Goeldi, Série Ciências da Terra*, **7**:147-164.

Barros C.E.M, Dall'Agnol R., Vieira E.A.P., Magalhães M.S. 1995. Granito Central da Serra dos Carajás: avaliação do potencial metalogenético para estanho com base em estudos da borda oeste do corpo. *Boletim do Museu Paraense Emílio Goeldi, Série Ciências da Terra*, **7**:93-123.

Belousova E.A. & Griffin W.L. 2002. Igneous zircon: Trace element composition as an indicator of source rock type. *Contribution to Mineralogy and Petrology*, **143**:602-622.

Blevin P.L. & Chappell B.W. 1992. The role of magma sources, oxidation states and fractionation in determining the granite metallogeny of eastern Australia. *Transactions of the Royal Society of Edinburgh: Earth Sciences*, **83**:305-316.

Blevin P.L. & Chappell B.W. 1995. Chemistry, origin and evolution of mineralized granites in the Lachlan Fold Belt, Australia: The metallogeny of I- and S-type granites. *Economic Geology*, **90**:1604-1619.

Blevin P.L., Chappell B.W., Allen C.M. 1996. Intrusive metallogenic provinces in eastern Australia based on granite source and composition. *Transactions of the Royal Society of Edinburgh: Earth Sciences*, **87**:281-290.

Dall'Agnol R., Rämö O.T., Magalhães M.S., Macambira M.J.B. 1999a. Petrology of the anorogenic, oxidized Jamon and Musa granites, Amazonian Craton: Implications for the genesis of Proterozoic A-type granites. *Lithos*, **46**:431-462.

Dall'Agnol R., Scaillet B., Pichavant, M. 1999b. An experimental study of a lower Proterozoic A-type granite from the eastern Amazonian Craton, Brazil. *Journal of Petrology*, **40**:1673-1698.

Dall'Agnol R., Teixeira N.P., Rämo O.T., Moura C.A.V., Macambira M.J.B., Oliveira D.C. 2005. Petrogenesis of the Paleoproterozoic rapakivi A-type granites of the Archean Carajás metallogenic province, Brazil. *Lithos*, **80**:101-129.

Dall'Agnol R., Oliveira M.A., Almeida J.A.C., Althoff F.J., Leite A.A.S., Oliveira D.C., Barros C.E.M. 2006. Archean and Paleoproterozoic granitoids of the Carajás metallogenetic province, eastern Amazonian Craton. *In:* Dall'Agnol R., Rosa-Costa L.T., Klein E.L (eds.). Symposium on magmatism, crustal evolution, and metallogenesis of the Amazonian Craton. Abstracts volume and field trips guide, Belém, PRONEX-UFPA/SBG-NO, p. 99-150.

Fowler A., Prokoph A., Stern R., Dupuis C. 2002. Organization of oscillatory zoning in zircon: Analysis, scaling geochemistry, and model of a zircon from Kipawa, Quebec, Canada. *Geochimica et Cosmochimica Acta*, **66**:311-328.

Dall'Agnol R. & Oliveira D.C. 2007. Oxidized, magnetite-series, rapakivi-type granites of Carajás, Brazil: Implications for classification and petrogenesis of A-type granites. *Lithos*, **93**:215-233.

Guimarães F.V., Dall'Agnol R., Almeida J.A.C., Oliveira M.A. 2010. Caracterização geológica, petrográfica e geoquímica do Trondhjemito Mogno e Tonalito Mariazinha, Terreno Granito-Greenstone mesoarqueano de Rio Maria - SE do Pará. *Revista Brasileira de Geociências*, **40**:196-211.

Hanchar J.M. & Miller C.F. 1993. Zircon zonation patterns as revealed by cathodoluminescence and backscattered electron images: Implications for interpretation of complex crustal histories. *Chemical Geology*, **110**:1-13.

Heaman L.M., Bowins R., Crocket J. 1990. The chemical composition of igneous zircon suites: Implications for geochemical tracer studies. *Geochemical et Cosmochimica Acta*, **54**:1597-1607.

Hanchar M. & Hudnick R.L. 1995. The application of cathodoluminescence and back-scattered electron imaging to dating zircons from lower crustal xenoliths. *Lithos*, **36**:289-303.

Horbe M.A. 1998. *Petrografia e geoquímica do Granito Pojuca, Serra dos Carajás-PA*. Dissertação de Mestrado. Centro de Geociências. Universidade Federal do Pará, Belém, 153 p.

Hoskin P.W.O. & Ireland T.R. 2000. Rare earth element chemistry of zircon and its use as a provenance indicator. *Geology*, **28**:627-630.

Huhn S.R.B., Santos A.B.S., Amaral A.F., Ledsham E.J., Gouveia J.L., Martins L.B.P., Montalvão R.M.G., Costa V.G. 1988. O terreno granito-greenstone da região de Rio Maria - Sul do Pará. *In:* SBG, Congresso Brasileiro de Geologia, 35, Belém, *Anais* **3**:1438-1453.

Ishihara S. 1981. The granitoid series and mineralization. *Economic Geology*, **75**:458-484.

Juliani C. & Fernandes C.M.D. 2010. Well-preserved Late Paleoproterozoic volcanic centers in the São Félix do Xingu region, Amazonian Craton, Brazil. *Journal of Volcanology and Geothermal Research*, **191**:167-179.

Kempe U., Gruner T., Renno A.D., Wolf D., René M. 2004. Discussion on Wang *et al.* (2000) "Chemistry of Hf-rich zircons from the Laoshan I- and A-type granites, Eastern China". *Mineralogical Magazine*, **64**:867-877.

Krinsley D.H. & Manley C.R. 1989. Backscattered electron microscopy as an advanced technique in petrography. *Journal of Geological Education*, **37**:202-209.

Lamarão C.N., Dall'Agnol R., Silva J.S., Soledade G.L. 2010. Morphological and compositional variation in zircons of tin-specialized Paleoproterozoic A-type granites of the Amazonian Craton: Metallogenic implications. *In:* O. Tapani Ramo, Sari Lukkari, Aku Heinonen (eds.), International Conference on A-type granites and related rocks though time (IGCP-510), Helsinki, Finland. Helsinki University, Department of Geosciences and Geography. Helsinki University Print, Abstract Volume.

Lamarão C.N., Dall'Agnol R., Soledade G.L., Silva J.S. 2007. Variações composicionais de zircão em granitos anorogênicos proterozóicos do Cráton Amazônico: Implicações metalogenéticas. *Revista Brasileira de Geociências*, **37**:693-704.

Lamarão C.N., Pinho S.C.C., Paiva Junior A.L., Toro M.A.G. 2012. Mineralogy and geochemistry of the Paleoproterozoic, tin-mineralized Bom Jardim Granite of the Velho Guilherme Suite, eastern Amazonian Craton. *Journal of South American Earth Sciences*, **38**:159-173.

Leite A.A.S., Dall'Agnol R., Macambira M.J.B., Althoff F.J. 2004. Geologia e geocronologia dos granitóides arqueanos da região de Xinguara (PA) e suas implicações na evolução do Terreno Granito-Greenstone de Rio Maria. *Revista Brasileira de Geociências*, **34**:447-458.

Macambira M.J.B. & Lafon J.M. 1995. Geocronologia da Província Mineral de Carajás: Síntese dos dados e novos desafios. *Boletim do Museu Paraense Emílio Goeldi, Série Ciências da Terra*, **7**:263-287.

Machado N., Lindenmayer Z.G., Krogh T.E., Lindenmayer D. 1991. U-Pb geochronology of Archean magmatism and basement reactivation in the Carajás area, Amazon shield, Brazil. *Precambrian Research*, **49**:329-354.

Oliveira M.A., Dall'Agnol R., Althoff F.J., Leite A.A.S. 2009a. Mesoarchean sanukitoid rocks of the Rio Maria Granite-Greenstone Terrane, Amazonian Craton, Brazil. *Journal of South American Earth Sciences*, **27**:146-160.

Oliveira D.C., Dall'Agnol R., Barros C.E.M., Oliveira M.A. 2009b. Geochemistry and magmatic evolution of the Paleoproterozoic, anorogenic A-type Redenção granite of the Jamon Suite, eastern Amazon Craton, Brazil. *Canadian Mineralogist*, **47**:1441-1468.

Owen M.R. 1987. Hafnium content of detrital zircons: A new tool for provenance study. *Journal of Sedimentary Petrology*, **57**:824-830.

Paiva Júnior A.L. 2009. Geologia, petrografia, geocronologia e geoquímica do Granito anorogênico Seringa, Província Mineral de Carajás, SSE do Pará, MS Dissertation, Programa de Pós-graduação em Geologia e Geoquímica, Instituto de Geociências, Universidade Federal do Pará, Belém, 120 p.

Paterson B.A., Stephens W.E., Herd D.A. 1989. Zoning in granitoid accessory minerals as revealed by backscattered electron imagery. *Mineralogical Magazine*, **53**:55-62.

Paterson B.A., Stephens W.E, Rogers G., Williams I.S, Hinton R.W, Herd D.A. 1992. The nature of zircon inheritance in two granite plutons. *Transactions of the Royal Society of Edinburgh: Earth Sciences*, **83**:459-471.

Pinho S.C.C. 2005. Petrografia e geocronologia da borda ENE do Granito Serra da Queimada e da borda SE do Granito Bom Jardim, Província Estanífera do Sul do Pará. Trabalho de Conclusão de Curso, Instituto de Geociências, Universidade Federal do Pará, Belém, 41 p.

Pupin J.P. 2000. Granite genesis related to geodynamics from Hf-Y in zircon. *Transactions of the Royal Society of Edinburgh: Earth Sciences*, **91**:245-256.

Rämö O.T., Dall'Agnol R., Macambira M.J.B., Leite A.A.S., Oliveira D.C. 2002. 1.88 Ga oxidized A-type granites of the Rio Maria region, eastern Amazonian Craton, Brazil: Positively anorogenic! *Journal of Geology*, **110**:603-610.

Rios F.J., Villas R.N., Dall'Agnol R. 1995. O granito Serra dos Carajás: 1. Fácies petrográficas e avaliação do potencial metalogenético para estanho no setor norte. *Revista Brasileira de Geociências*, **25**:20-31.

Rios F.J., Villas R.N., Fuzikawa K. 2003. Fluid evolution in the Pedra Preta wolframite ore deposit, Paleoproterozoic Musa granite, eastern Amazonian Craton, Brazil. *Journal of South American Earth Sciences*, **15**:787-802.

Santos J.O.S., Hartmann L A., Gaudette H.E., Groves D.I., McNaughton N.J., Fletcher I.R. 2000. A new understanding of the Provinces of the Amazon Craton based on integration of field and U-Pb and Sm-Nd geochronology. *Gondwana Research*, **3**:453-488.

Souza Z.S., Potrel A., Lafon J.-M., Althoff F.J., Pimentel M.M., Dall'Agnol R., Oliveira C.G. 2001. Nd, Pb and Sr isotopes of the Identidade Belt, an Archean greenstone belt of the Rio Maria region (Carajás Province, Brazil): Implications for the Archaean geodynamic evolution of the Amazonian Craton. *Precambrian Research*, **109**:293-315.

Tassinari C.C.G. & Macambira M.J.B. 2004. Evolução tectônica do Cráton Amazônico. *In:* Mantesso-Neto V., Bartorelli A., Carneiro C.D.R., Brito Neves B.B. de. (orgs.) *Geologia do Continente Sul Americano:* Evolução da obra de F.F.M. de Almeida. São Paulo, Beca, p. 471-486.

Teixeira N.P., Bettencourt J.S., Dall'Agnol R., Moura C.A.V., Fernandes C.M.D., Pinho S.C.C. 2005. Geoquímica dos granitos paleoproterozóicos da Suíte Granítica Velho Guilherme, Província Estanífera do Sul do Pará. *Revista Brasileira de Geociências*, **35**:217-226.

Teixeira N.P., Betencourt J.S., Moura C.A.V., Dall'Agnol R., Macambira E.M.B. 2002. Pb-Pb geochronology and Sm-Nd isotopic composition of the Velho Guilherme Intrusive Suite and volcanic rocks of the Uatumã Group, south-southeast Pará - Brazil. *Precambrian Research*, **119**:257-275.

Uher P., Breiter K., Klecka M., Pivec E. 1998. Zircon in highly evolved Hercynian Homolka granite, Moldanubian zone, Czech Republic: Indicator of magma source and petrogenesis. *Geologica Carpathica*, **49**:151-160.

Vasquez L.V., Rosa-Costa L.R., Silva C.G., Ricci P.F., Barbosa J.O., Klein E.L., Lopes E.S., Macambira E.B., Chaves C.L., Carvalho J.M., Oliveira J.G., Anjos G.C., Silva H.R. 2008. Geologia e Recursos Minerais do Estado do Pará: Sistema de Informações Geográficas - SIG: Texto explicativo dos mapas Geológico e Tectônico e de Recursos Minerais do Estado do Pará. Organizadores, Vasquez M.L., Rosa-Costa L.T. Escala 1:1.000.000. Belém: CPRM.

Vavra G., Gebauer D., Schmid R., Compston W. 1996. Multiple zircon growth and recrystallization during polyphase Late Carboniferous to Triassic metamorphism in granulites of the Ivrea zone (Southern Alps): An ion microprobe (SHRIMP) study. *Contribution to Mineralogy and Petrology*, **122**:337-358.

Villas R.N.N. 1999. Granito Pojuca, Serra dos Carajás (PA): composição mineralógica, química mineral e controles químicos da alteração hidrotermal. *Revista Brasileira de Geociências*, **29**:393-404.

Wang R.C., Fontan F., Xu S.J., Chen X.M., Monchoux P. 1996. Hafnian zircon from the apical part of the Suzhou granite, China. *Canadian Mineralogist*, **34**:1001-1010.

Wang R.C., Zhao G.T., Lu J.J., Chen X.M., Xu S.J., Wang D.Z. 2000. Chemistry of Hf zircons from the Laoshan I- and A-type granites, eastern China. *Mineralogical Magazine*, **64**:867-877.